

Review

# Current Status and Challenges of Powder Bed Fusion-Based Metal Additive Manufacturing: Literature Review

Naol Dessalegn Dejene \*  and Hirpa G. Lemu 

Department of Mechanical and Structural Engineering and Materials Science, Faculty of Science and Technology, University of Stavanger, N-4036 Stavanger, Norway

\* Correspondence: nd.dejene@stud.uis.no

**Abstract:** Powder bed fusion (PBF) is recognized as one of the most common additive manufacturing technologies because of its attractive capability of fabricating complex geometries using many possible materials. However, the quality and reliability of parts produced by this technology are observed to be crucial aspects. In addition, the challenges of PBF-produced parts are hot issues among stakeholders because parts are still insufficient to meet the strict requirements of high-tech industries. This paper discusses the present state of the art in PBF and technological challenges, with a focus on selective laser melting (SLM). The review work focuses mainly on articles that emphasize the status and challenges of PBF metal-based AM, and the study is primarily limited to open-access sources, with special attention given to the process parameters and flaws as a determining factor for printed part quality and reliability. Moreover, the common defects due to an unstrained process parameter of SLM and those needed to monitor and sustain the quality and reliability of components are encompassed. From this review work, it has been observed that there are several factors, such as laser parameters, powder characteristics, material properties of powder and the printing chamber environments, that affect the SLM printing process and the mechanical properties of printed parts. It is also concluded that the SLM process is not only expensive and slow compared with conventional manufacturing processes, but it also suffers from key drawbacks, such as its reliability and quality in terms of dimensional accuracy, mechanical strength and surface roughness.

**Keywords:** additive manufacturing; selective laser melting; defects; process parameter; powder bed fusion; surface roughness; porosity; microstructure; residual stress



**Citation:** Dejene, N.D.; Lemu, H.G. Current Status and Challenges of Powder Bed Fusion-Based Metal Additive Manufacturing: Literature Review. *Metals* **2023**, *13*, 424. <https://doi.org/10.3390/met13020424>

Academic Editor: Zhanyong Zhao

Received: 22 January 2023

Revised: 11 February 2023

Accepted: 16 February 2023

Published: 18 February 2023



**Copyright:** © 2023 by the authors. Licensee MDPI, Basel, Switzerland. This article is an open access article distributed under the terms and conditions of the Creative Commons Attribution (CC BY) license (<https://creativecommons.org/licenses/by/4.0/>).

## 1. Introduction

A new class of technology known as additive manufacturing (AM), commonly referred to as three-dimensional (3D) printing, is concerned with the direct production of physical items from computer-aided design (CAD) models utilizing a layered manufacturing process. A revolutionary change from craft to mass production occurred in the manufacturing paradigm prior. AM's arrival resulted in a fresh paradigm shift away from mass manufacturing and toward mass customization [1]. AM has grown exponentially because of its crucial role in the fourth industrial revolution [2]. Due to that, AM has become a key technology for fabricating customized products owing to its ability to create complex objects with advanced attributes (new materials, shapes) [3], near net shape, and buy-to-fly ratio [4,5]. According to the consensus among researchers and the industrial community's findings, metals based on AM technologies have tremendous application potential that cannot be matched by traditional manufacturing technologies [6], and metal AM is a promising technology in the next generation of the manufacturing process [7]. Moreover, the AM market, though small compared to traditional manufacturing, has grown rapidly, which is shown in Figure 1 of Ref. [1]. According to Koutiri et al. [8], since 2003, there has been a 42% increase in parts produced by AM. Wohler's report in the 2017–2018 reporting period [1] also reported that the overall 3D printing industry grew by 21%. Moreover, according to

the Wohler's association in 2020, an industrial insight report on the AM market, the average annual growth of the AM market was predicted to be over 20% in the next five years [9].

The ISO/ASTM 529000:2015 standard has categorized the AM methods into seven main groups, including binder jetting, directed energy deposition, material extrusion, powder bed fusion, sheet lamination and vat photopolymerization [10–12]. PBF method is widely employed in a variety of industrial areas, including the aerospace, energy, transportation [13,14], biomedical, automobile and jewelry industries [8,15–17]. PBF is the focus of this paper, and details are given in Section 3.

Quality and reliability are major concerns in state-of-the-art Industry 4.0 technologies, including AM [18]. AM technologies have recently gained more attention due to their ability to manufacture complex parts, so the quality and reliability of AM is an emerging area. The challenges of PBF-produced parts have become a hot issue among stakeholders. Tapia et al. [6] demonstrated a consensus among experts and stakeholders in the aerospace, healthcare, and automotive fields that metallic AM parts are still not sufficient to meet their stringent requirements. For successful adoption, it is necessary to have a comprehensive understanding of the materials ecosystem in AM. This paper discusses the present state of the PBF process and technological challenges, with a focus on SLM. Decisively escaped discussing all types of PBF processes, instead focused on SLM and slightly stating electron beam powder bed fusion (EB-PBF).

## 2. Materials and Methods

In this review work, the literature coverage considered is comprised of open scientific sources published mainly in the last 10 years. To obtain sufficient coverage of the works reported on the topic of the PBF-based AM process, we used the following scientific databases to search through the literature: scientific.net, Scopus, Elsevier, Science Direct, web of science, Google scholar, springer, semantic scholar, PubMed, JSTOR, DOAJ, MPDI, research gate, SAGE, BASE, SCISPACE, Taylor & Francis and others. The search keywords used in English language were additive manufacturing, powder bed fusion, selective laser melting, defects, process parameters, quality, surface roughness, porosity, microstructure, residual stress, etc. Other descriptive terms were also used in some cases to be specific with the objective of the review.

## 3. Powder Bed Fusion—Based Metal Additive Manufacturing Process

PBF is a group of AM technologies where an energy source is used to selectively bind or melt powder particles to build parts layer by layer to the desired geometry [15]. The first PBF process, selective laser sintering (SLS), was developed at the University of Texas [2,12,19,20]. According to Ahmadi et al. [21], SLM began in 1995 at the Fraunhofer Institute ILT in Aachen, Germany.

All other PBF processes significantly change the latter basic approach in one or more ways to improve machine productivity. The basic schematic representation of the PBF process is illustrated in Figure 1. PBF is widely applied and possibly the most evolved AM technology available [22]. According to Vafadar et al. [23], 54% of the metal AM market belongs to PBF processes as of 2020. Korpela et al. [24] stated PBF-process is the most evolved metal AM technology to produce engineering components. The PBF machine manufacturer has their own specific commercial names, such as SLS, direct metal laser sintering (DMLS) and SLM, which is also known as laser powder bed fusion (L-PBF) or electron beam melting (EBM) [13,23–27]. Although some systems have the word “sintering” in their names, the majority of metal PBF systems in use today completely melt the particles rather than sintering them [24,28].

Comparing the effectiveness of those PBF and other processes is currently becoming a research concern. For example, the PBF shares common parameters with directed energy deposition (DED). The PBF system utilizes a powder deposition method that consists of a recoating mechanism that spreads a powder layer onto a substrate plate and a powder reservoir. Once the powder is evenly distributed, PBF uses thermal energy from a heat

source (laser or an electron beam) to trace the geometry of an individual layer of slices from a 3D model on the powder bed's surface [29]. DED can use the same source of energy and feedstock as PBF. However, DED deposits a melted material feedstock through a nozzle onto a surface [30]. The similarity between DED and PBF under the same source of energy becomes an interesting concern. DED has a high deposition rate and is preferable for larger component manufacturing due to the slower process of PBF [31]. PBF methods have an advantage over DED methods in producing parts with higher resolution and quality [30]. Babuska et al.'s [7] findings strengthen the aforementioned statements, where the mechanical performance of Fe-Co components is produced by PBF and DED under a laser beam. The part L-PBF was characterized as high strength (500–550 MPa) and high ductility (35%), while L-DED results in low strength (200–300 MPa) and low ductility (0–2.7%). Even though there are fundamental manufacturing approaches, the process parameters involved at different levels are not explained in the study.

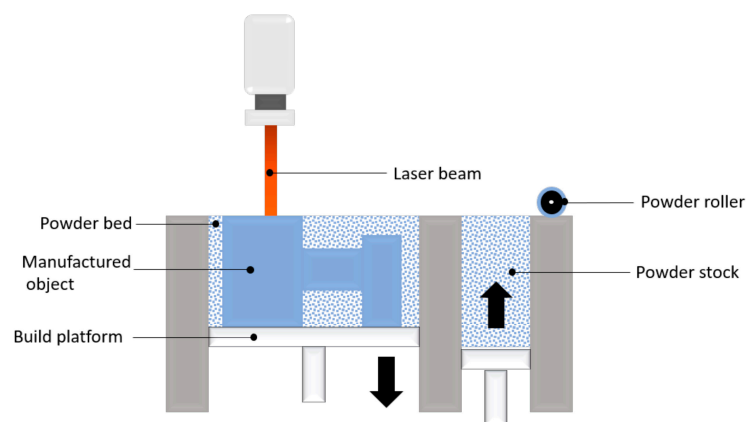


**Figure 1.** Schematic representation of PBF (Reused from [32] with permission in accordance with Creative Common CC BY license, open access).

The comparison among the PBF sub-categories is also another concern of the continuous improvements in R&D. The printing process of both L-PBF and EB-PBF is nearly the same [4] or a similar process [33]. However, there are several differences that need consideration as they affect the quality of the final components. Basically, EB-PBF was introduced to overcome the challenges of L-PBF, such as power and speed [15]. EB-PBF uses a high-energy electron beam 3000 W [15] or (~3500 W) [34]) and proceeds in a vacuum to control the oxidation of highly reactive metals like titanium and magnesium [19,20]. The presence of a vacuum atmosphere in EB-PBF favors slower cooling rates [14], which leads to lower residual stress [4,14,35]. However, EB-PBF suffers from poorer dimensional accuracy [29,36] and surface roughness [29,37] and is limited to only conductive metals [4,19]. Thus, it is comparatively less applied to the current technology in the industry. In contrast, L-PBF has a relatively broader application due to its capacity to produce fine-size features (i.e., to small pool size) and intricate features [4]. L-PBF uses lower power (100–1000 W) [14,38], relatively good dimensional accuracy and roughness [14,39]. The challenges of L-PBF are high porosity due to the presence of inert gas or nitrogen [40], fast cooling rate that leads to high residual stress [14] and a slow scanning speed [19] compared to EB-PBF. However, L-PBF (SLM) emerges as a leading candidate to manufacture mission-critical applications [41–43], such as aerospace and defense applications [44]. Therefore, the focus of this study is principally on the SLM, which is currently the most used metal AM technique for fabricating parts.

#### 4. Process Parameters in Powder Bed Fusion-Based Metal Additive Manufacturing

As mentioned earlier, PBF is possibly the most evolved AM technology. However, the production process is still expensive and slow compared to conventional manufacturing. Moreover, the components are typically semi-finished and need post-processing. According

to Ladani et al. [15], the most interesting aspect of PBF-AM is the possibility of the potential control of final products through a bottom-up approach; i.e., microstructure, flaws and other properties can be controlled through the process by intelligently varying the parameters. Several authors agree on the primary contribution of process parameters to the formation of defects. Hence, monitoring the root causes of defects and controlling them provides important insights into enhancing the quality of final products. Numerous researchers stated the influential process parameters for SLM as laser input energy, powder material and scanning speed [45]. Murugan et al. [16] considered the layer thickness, scan speed, hatch spacing, size of the powder particles and orientation of the layer. Javidrad et al. [46] used scanning speed, laser power and hatching space to determine the effect of volume energy density (VED) on the microstructure of Inconel 625. From the process mapping, it is identified that the thermal gradients, melt pool size and residual stress are affected by the powder feed process [33,47].

As Ladani et al. [15] stated, the outcome of SLM largely depends on process parameters and the interplay of physical phenomena. The great desire of the manufacturing industry is to be more profitable through high production rates, low wastage, no defects and less effort. So, the significant contribution of process parameters to the final product is revealed via various studies. However, the parameters guaranteeing the highest production speeds are not disclosed with the best achievable accuracies. For example, layer thickness increases have a significant positive impact on building time and a negative impact on accuracy [24,40]. This implies that as the production rate increases, the desired quality decreases, so several process parameters need to be considered in SLM. However, some of those can be predicted in advance, while others are challenging to predict because they are generated through rigorous processes. Therefore, bottom-up monitoring and controlling process parameters are vital techniques. This review categorizes the aspects of the bottom-up process parameters sources under powder, laser, powder material, and printing chamber environment parameters, as shown in Figure 2.

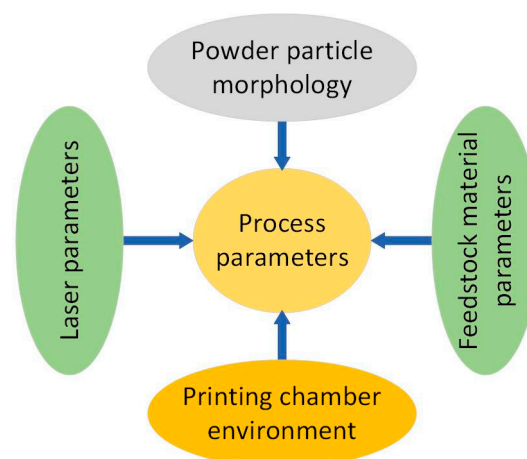


**Figure 2.** The source of process parameters for PBF-AM.

#### 4.1. Aspects of the Powder Particle Morphology

The PBF-based metal AM received attention from industries and R&D due to its rewards, high degree of customization and the minimal buy-to-fly ratio [5]. The hard materials that would be difficult by other manufacturing processes are some of the reasons why SLM tends to be selected. Moreover, SLM can produce complex feature parts, and powder can be reused. However, the SLM process came with additional properties of powder particle size distribution (PSD), shape, density, flowability and other powder morphology, which have considerable impacts on the qualities of components. Those parameters can be categorized as the single particle (shape, smoothness, PSD, impurities, composition, moisture, etc.) and bulk properties (apparent or bulk density, tap density, Hausner ratio,

flowability and physical properties) [48]. The parameters related to the powder morphology are the pre-defined or pre-process parameters. The powder morphologies, such as PSD and shape characteristics of individual particles, such as sphericity and uniformity, have significant effects on the bulk properties of powder as well as the final part. This is due to their critical impact on determining the optical penetration depth [49,50].

The single-particle morphology determines the conductivity due to the voids and level of connection among particles. This affects the penetration depth and leads to melting pool size and shape, which are responsible for the variability in part properties and several defects [49]. The bulk properties of powder particles, such as flowability, have various interrelated effects on the process [48]; a very small change in the PSD influences the flowability, which has been noted to impact packing density [51]. The flowability is reduced due to the satellite particles (<10–15  $\mu\text{m}$ ) connected to large particles impacting the packing density due to increased mechanical interlocking powder flows in SLM [40]. However, the fine grain size enables achieving better layer thickness, which improves surface roughness. According to Karapatis et al. [52], experimental results show the apparent density of thin powder layers increases from 53% to 63% of solid material when adding 30 vol % of fine powder to the coarse one. The mechanical performance improvements in steel components in the SLM process are due to refined microstructure by small particles [43]. This indicates the contribution of particle size in microstructure is also noticeable.

The material properties of components are extremely sensitive to pre-process parameters [53–55]. Spierings et al. [56] explored how three different powder granulations affect the mechanical characteristics, surface quality and part density of the produced SLM steel. The finding indicates the coarser particles result in a rougher surface and lower density. In the other case, fine particles are easily melted and favor good part density and surface quality, whereas large particles have the benefits of ductility, mechanical strength, hardness and toughness [57]. The flowability, which is the effect of both fine and large particles, impacts layer-to-layer variation in parts, and as the powder size increases, the yield strength and ultimate tensile strength (UTS) increase [49,51,58]. This reinforces that PSD has a concern with repeatability in the material properties of produced parts. Ladani et al. [15] mentioned that powder feedstock quality has a direct effect on the quality of fabricated parts and the repeatability of the process. Therefore, the PSD and other morphologies of powder have various effects on the parts, such as repeatability.

The powder particle source of challenges can be from the powder production techniques to the part manufacturing. However, there is inadequate coverage in the literature on the powder production techniques' improvement with the alignment of the PBF process. Powders prepared with different methods also showed different mechanical properties on the components due to the difference in their microstructure [15]. Samples fabricated using gas atomized (GA) powders showed higher microhardness than the samples prepared using mechanically alloyed plasma spheroidized (MAPS) powders with almost similar composition [15,59]. Sanaei et al. [60] find feedstock material as the first source of defects based on the atomization process and whether it carries entrapped gas. In addition, there are claims that the overestimation of the SLM material utilization is 100%. It has been reported that a 95% material efficiency is more reasonable [61]. So, it is crucial to realize how laser heat affects recycled metal powder and in what way that processing affects the final parts' microstructural and mechanical properties [62]. The impurities and powder recycling are keen aspects of monitoring the qualities of the part as bottom-up controlling. The leftover powder from each build is recycled, then returned to the system for further use. However, the powder can be exposed to air during handling, and hence, the formation of surface moisture and oxides is possible [62]. In addition, as one major aspect, the environment of the SLM processing chamber is very important to fabricate oxide-free parts.

Despite using protective inert environments and a shielding inert gas flow to limit the oxygen content in the working chamber, there is always a chance of a small percentage of unwanted oxygen content (~0.1–0.2%) present during the SLM process [63]. Oxygen existing in the surrounding atmosphere entrapped inside the powder particles causes

various defects like porosity, void formation and mechanical properties [16,40,57]. Moreover, considering the percentage of the recycled, as well as the number of recycling times, additional unseen characteristics of parts will be revealed. Lewis [5] addressed the effects of powder reuse PSD, the aspect ratio of particle morphology and flowability. However, the number of recycling is not addressed as there is a high chance of repetition in the SLM to be cost-effective.

The comparison of sieved recycled and fresh powder of AlSi10Mg microstructure was conducted, and slightly similar results were obtained [62–64]. However, the experimental work considered a limited number of recycled powders. The production of high-quality and fully dense components generally depends heavily on the grain shape, PSD, surface morphology and overall purity of metallic and alloying elements.

#### 4.2. Aspects of the Laser Process Parameters

In addition to the powder particle morphology, the SLM parts are sensitive to printing process parameters (e.g., beam size, power, scan rate and others) [54,65]. The SLM shares common parameters with seam welding [25,66], so most of the descriptions are taken analogically in different studies. Therefore, the defects that occur due to unrestrained process parameters in micro welding, such as keyholes that can be avoided by expanding the beam size [67], are expected in SLM.

The interaction of the laser and the powder is a complex phenomenon due to multiple phase changes and variable absorbance [27,49,57,68]. That is due to the powder morphology and the rapid timescale interaction with the focused nature of a laser spot on microscopic spatial scales. Even when operating on these small scales, minor perturbations can have a significant effect [49]. Therefore, the factors affecting energy absorption and quality of components are the beam spot size, the shape of the deposit geometry and protective gases [27]; this is due to their impacts on the size and shape of the melt pool [33,54]. Mudge et al. [69] indicated that the laser spot size needs to increase with powder feed to increase the deposition rate, which increases production volume [42]. However, doing that would lead to a coarse surface finish due to the increase in melt pool size. The size and shape of the melt pool affect the mechanical properties of the part, i.e., the formation of porosity and rough surface [49,70,71]. Melt pool size and shape are considered selection factors for other parameters. For instance, Aboulkhair et al. [71] considered melt pool size and shape for Ti64 related to forming pores and surface conditions. They suggested the operator find optimum values of other parameters because the measured porosity result shows an increase at too large or a decrease at too small a beam spot size [33].

Most of the parameters in the laser aspects are interrelated and too complex to figure out as they are very fast interactions with powder morphology timescales. However, energy density or specific energy encapsulates all other characteristics in a single variable. The proper energy density is critical for the melting of materials [26]. The energy density can be described by its spot size, pulse duration and frequency [62]. The fluctuation of energy density causes a repeatability problem in SLM as an inconsistent melt pool has effects, such as excess vaporization, that could occur from the transient higher energy levels [49].

The effectiveness of energy density can be affected by the morphology of powder [57] and scanning-related or printing chamber parameters. For instance, increases and decreases in scanning cause the formation of irregular and metallurgical morphology porosity, respectively [71]. The other scanning-related parameters include the scan speed, scan spacing and scan pattern [49]. There are also printing chamber-related factors, such as atmosphere (inert gas), oxygen level and chamber pressure [72], as well as temperature-related parameters (powder bed temperature, powder bed feeder and temperature uniformity) [49]. Adjusting the process parameters for the powders, chamber environment and laser, one could possibly alter the cooling rate and melt pool size. The important relation is that the quality of the final part is the function of the involving process parameters from all aspects. Ladani et al. [15] asserted the final microstructure of the part is a function of global-level parameters such as build atmosphere, build orientation, scanning strategy and

hatch spacing. This infers that the critical combination of those global process parameters can contribute to the quality of the final part.

#### 4.3. Aspects of the Feedstock Material-Related Parameters

Both in traditional manufacturing and AM, feedstock materials are one of the most vital factors in the quality of the finished product. Reduced mechanical qualities or even premature failure of the manufactured product could be caused by the poor quality of raw materials. In principle, all materials that can be melted and re-solidified can be used in the PBF process as feedstock [12]. According to Gibson et al. [19], any metal that can be welded or cast could be used in the SLM process. That is due to the similarities of involving process parameters [62]. However, the generalization of feedstock material selection for SLM based on their characteristics of weldability and castability as a good candidate for SLM does not have a strong scientific background due to the existence of huge differences between welding and casting with the SLM process. Aboulkhair et al. [62] investigated the difference associated with the solidification rate of both the SLM and casting process. The finding shows the solidification rate of the SLM process is much steeper than the casting process. Various mechanical properties and quality indicators, such as microstructures, are affected by the solidification process. According to Wu et al. [73], conventional processing such as welding and casting yields a coarse microstructure compared to SLM. Siddique et al. [74] reported the yield strength of an SLM AlSi12 is four times that of the sand-cast alloy, which they attributed to the fine microstructure. This indicates there could be variables that affect the microstructure of the part, possibly related to the solidification rate. Moreover, the feedstock format used in the case of SLM is powder, while welding uses bulk or wire that affects the laser power absorption behaviors, which is quite similar to the statement under the powder morphology aspect.

Furthermore, the materials repeatedly solidify and melt during re-scanning or re-melting in SLM, which is different from the condition that the same material will go through during welding. Therefore, the laser radiation can affect the alloying elements [61], which will have another impact on the final part, so it is crucial to develop novel alloy systems that are well suited for the SLM in terms of the desirable physical and chemical properties. However, only a few alloys, such as AlSi10Mg, TiAl6V4, CoCr and Inconel 718, are currently the most important and can be successfully printed, claimed by Martin et al. [17] in their study. The majority of more than 5500 alloys in use today cannot be additively manufactured because the melting and solidification dynamics during the printing process led to intolerable microstructures with large columnar grains and periodic cracks [17]. Understanding a material's thermal behavior during SLM is crucial before beginning the experimental qualifying of the material to predict the microstructures and mechanical properties of the parts [62]. However, fusion-based AM of metallic components is a promising technology with plenty of benefits and applications. The challenge from a feedstock perspective is that each application scenario imposes unique requirements on the alloy properties. In this respect, fusion-based AM is still in its infancy, with many available materials not designed for fusion-based AM processes.

The metals used in both AM and conventional manufacturing need parallel consideration of the process parameters involved in the process, i.e., significant alterations to the quality of the part. Table 1 reveals some of the literature that reported the same material processed under different manufacturing process yields with different final part characteristics. It indicates the weakness of the generalization that materials used in welding or casting could be for SLM.

**Table 1.** Tensile properties of Ti-6Al-4V fabricated by different processes.

Response Parameters	Tensile Properties (Ti-6Al-4V)					Units
	SLM	LBW	WAAM	Casting	EBW	
Ultimate tensile strength	1267 [68,75]	974 [75]	988 [75]	976 [68]	967 [75]	MPa
Yield strength	1110 [68,75]	942 [75]	909 [75]	847 [68]	922 [75]	MPa
Fracture tensile strain	7.28 [68,75]	10.03 [75]	7.5 [75]	5.1 [68]	9.7 [75]	%
Response parameters	Hardness and compressive properties (CP-Ti) [68]				Units	
	LPBF	55% Cold rolled	Casting			
Hardness	261	268	210		VH	
Compressive strength	1136	900	820		MPa	
Maximum strain	51	35	60		%	

EBW: Electron beam welding, WAAM: Wire arc additive manufacturing, LBW: laser beam welding, VH: Vickers hardness.

### 5. Powder Bed Fusion Additive Manufacturing Process Parameters and Defects

SLM has a unique ability to efficiently make complex shaped, hollow, thin-walled, or slender parts. The ability to produce a functional part and near-net shape using SLM without post-processing, i.e., machine finishing, would be an ideal use of the SLM process. However, finish machining operations are required to guarantee part assembly and the desired surface quality [76]. For instance, the milling operation, which is a commonly used machining operation for the post-processing of additively produced parts, often encounters challenges due to the anisotropic and crystalline textures. As a result, examining the effects of SLM parameters on the cutting force and anisotropy of the Inconel 718 parts has been the subject of recent research [77]. According to Perez-Ruiz et al. [77], post-machining processes are still necessary to improve dimensional and surface quality, particularly in low-stiffness components. To increase the stiffness of SLM components, they suggested an iterative design process to obtain improved surface roughness and cutting force for thin-walled bent ducts.

The process parameters of the PBF process have great impacts on the final products. Understanding AM defects is essential for failure analysis, defect-based mechanical performance modeling and the structural integrity of load-bearing components [60]. The parameters could be from the powder morphology, laser related, the feedstock material or the printing chamber environments. Currently, the main challenge of PBF is a complete understanding of the relation between the processing parameters and the final quality of components [68]. As mentioned in an earlier section, the factors from different aspects contributed to the final qualities. The output parameters represent the quality of SLM products manifested in the form of geometry, microstructure, surface texture (lay, roughness, waviness), porosity, cracking, distortion, delamination, balling, residual stress [27,43] and others. According to Maurya et al. [27], the defects in AM are common, and that is due to the process parameter; optimization is very important. Therefore, determining which parameters are involved in the formation of specific defects is important.

#### 5.1. Microstructural Defects in PBF-AM Fabricated Parts

The microstructure of the part is vital due to its significant impact on corrosion resistance [78], fracture, toughness [79], ductility [80], thermal conductivity [81] and other prominent properties [13]. Therefore, having consistent microstructure in additively manufactured parts is a big concern. The microstructure is the function of various process parameters, and a variety of microstructures can be produced under different parameters. The fact that each layer is created by partially melting and solidifying the previous layer adds complexity to the SLM process. In addition, SLM experiences a fast cooling rate of  $10^4$  to  $10^6$  K/s [46] due to the substantial temperature gradient and even leads to cracks owing to rapid shrinkage [82].

The role of process parameters in forming a variety of microstructures is significant. For instance, laser power, scan speed, layer thickness, hatching distance, scanning strategy and others show different microstructures, including single crystalline-like microstructures, crystallographic lamellar microstructures and polycrystalline microstructures [83]. Crystal textures cause the anisotropy of mechanical properties such as Young's modulus, yield stress and wear resistance [84]. Anisotropic microstructures are commonly developed based on the cooling direction within a melt pool. On the other hand, SLM is highly effective at controlling the crystallographic texture of a wide range of metallic materials, from randomly oriented polycrystalline to single crystalline-like microstructures. The single-crystal-like metal structures are applied to fabricate nearly totally dense tungsten parts with a relative density of 99.1% by tuning the laser process parameters, which is the greatest value yet reported [85]. However, suppression of the occurrence of compositional supercooling is required to obtain a single crystal [84].

Several authors considered the impacts of different process parameters on the condition of the microstructure of metal-based PBF. For instance, Niendorf et al. [86] produced a highly anisotropic microstructure of 316L stainless steel with strong texture by variation of the laser power at the value of 400 and 1000 W, average PSD of 40  $\mu\text{m}$  at 50  $\mu\text{m}$  and 150  $\mu\text{m}$  layer thickness. The use of a 1000 W high-energy laser system reveals a coarse and strongly textured microstructure. The significance of the other parameters (except for laser power at 100 W), such PSD and scanning speed, are not clearly described or emphasized. Martin et al. [17] indicated the contribution of PSD on the formation of microstructures, and the parameters of powder have a significant contribution to altering the form of microstructures. Even the introduction of nanoparticles to SLM is part of the evolution of an isotropic microstructure with fine equiaxed grains [17]. The study on the Inconel 718 samples with layer thicknesses (20, 30, 40 and 50  $\mu\text{m}$ ) reveals that the lower the layer thickness, the denser and better the dimensional accuracy [87], which is marginally related to mechanical properties, i.e., microstructure.

Furthermore, several authors considered the energy density or specific energy density as the vital parameter to determine the microstructure of the SLM part. The relationship between specific energy density, microstructure, and corrosion resistance of the SLM specimens of CoCrMo under SLM was investigated [88]. The findings demonstrate that a higher specific energy density promotes columnar grain development and results in coarse grain size, and critical energy density is suggested. Energy density is dependent on other parameters, such as laser power and scanning speed, i.e., increasing scanning speed reduces line energy density [15]. This is due to local energy losses, such as the interaction of the beam with a different morphology of powder and hatching strategy. In addition, a higher beam current causes a loss in alloying elements from the original composition and forms defects in the microstructure. For instance, the research of Ge et al. [89] on Ti-47Al-2Cr-2Nb shows at 10 mA, there was a 15% loss of aluminum, and the microstructure also exhibited a variance with the beam current compared to raw powder composition, as shown in Table 2; the perspective microstructure is illustrated in Figure 3. Therefore, considering the melting point of alloying elements of feedstock materials while applying beam currents is critical.

**Table 2.** Chemical composition of as-built samples (atomic percentage) [89].

Sample No	Melting Beam Current (mA)	Ti	Al	Cr	Nb
1	4	45.25	50.48	2.17	2.10
2	6	55.63	39.71	2.08	2.58
3	8	58.13	37.43	1.62	2.82
4	10	61.85	33.50	1.47	3.19

In high-tech industries such as energy and aeronautics, some components need to be very lightweight without compromising their strength, which has a direct relation with the microstructure [90]. The microelement size, shape and topology design and optimization are becoming vital challenges, particularly in the manufacturing of skeletons with cavities,

which are the concern of additive manufacturing. Calleja-Ochoa et al. [90] proposed the use of “replicative” structures in various sizes and orders of magnitude to manufacture parts with minimum weight while maintaining the needed mechanical properties.

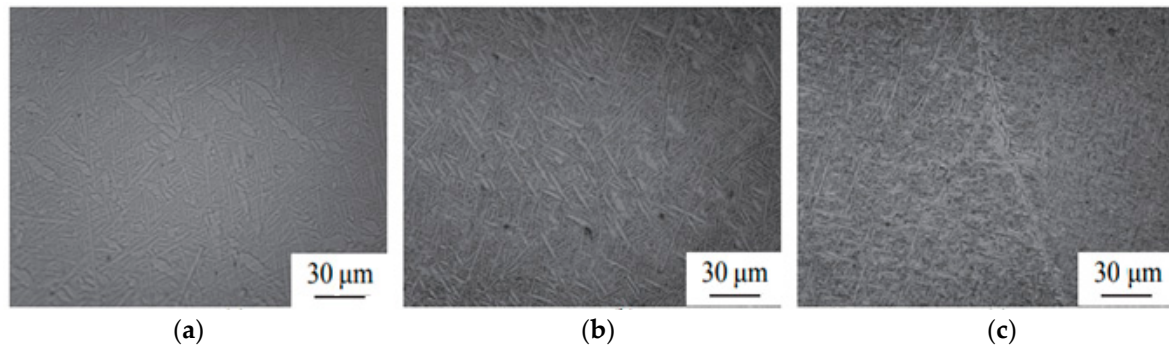


**Figure 3.** Optical microscopy in top region (a) Sample-2, (b) Sample-3 and (c) Sample-4 (Reused by permission form [89], License number 5462390275210).

In general, the literature shows that the microstructure is the actual concern of SLM, and scholars identified process parameters that need to be monitored separately. The property of the material under consideration is also essential since the dynamics of melting and solidification during the printing process result in intolerable microstructure and cracks, as already mentioned by Martin et al. [17]. However, there is small coverage with collective impacts that are related to laser, powder morphology, feedstock material and chamber condition.

### 5.2. Surface Roughness of PBF of Produced Parts

Surface texture is the geometrical irregularities or roughness that exist on the surface [57] and is influenced by different factors of SLM [27,43]. Surface quality is one of the unsolved problems in SLM [91]. The surface finish condition plays a key role in the mechanical, tribological and functional performance of SLM components [43]. For example, an increase in surface roughness tends to cause faster crack initiation, with a resulting decrease in fatigue performance [92].

The surface roughness of SLM parts is nearly four to five times of the machined surface. Therefore, addressing those responsible process parameters is the principal endeavor. From the powder morphologies, PSD, shape, smoothness, apparent density and flowability are some of the factors considered by various authors that have shown significant contributions to surface roughness [48,56,57,93]. The large particles inside layers could cause a rough surface because the volume of particles tends to form voids when they are removed in the finishing process [94]. The staircase is another source of a rough surface due to the layered nature of part construction, creating a stair-stepping effect that is heavily dependent on part orientation [95]. In addition to surface roughness, the staircase causes dimensional inaccuracy and volumetric error, as shown in Figure 4, where  $S_i$  is the contour area of  $i$ th layer.

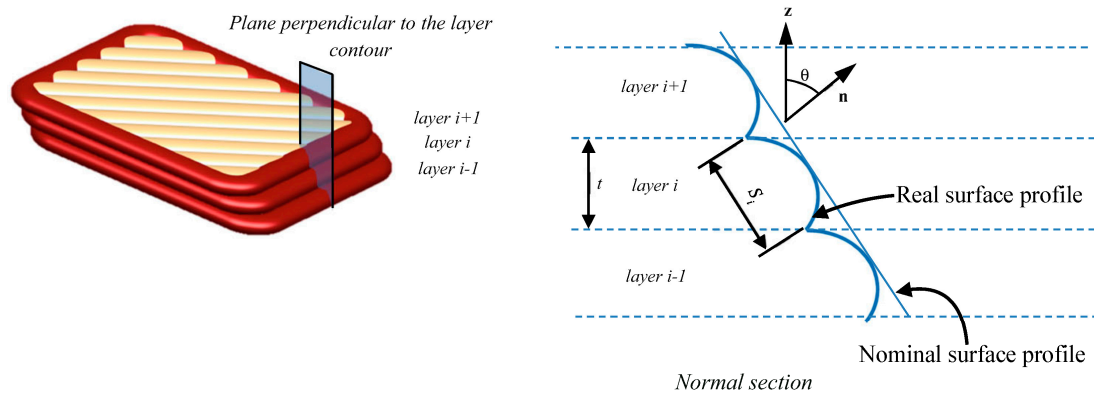


**Figure 4.** SLM process and staircase error (Reused from [96] with permission in accordance with Creative Common CC BY license, open access).

The other surface roughness challenge of SLM comes from the standard triangulation language (STL) file [97], as it is responsible for creating slice thickness that leads to a staircase effect on the part. The variation of surface roughness with the .STL file is given in Table 3. In the other case, the combined effect of the scanning speed and layer thickness study shows as both parameters increase, the surface roughness increases, which is given in Table 4. However, the study missed that layer thickness could be affected by the flowability of the powder. Poor powder flowability blocks the spreading of particles and affects the continuity of layer-led rough surfaces [43]. This implies the powder morphology, which determines the flowability status, has indirect impacts on the surface condition of the component.

**Table 3.** Surface roughness and deviation [97].

Sample	No. of Triangles	Ra [ $\mu\text{m}$ ]	Rz [ $\mu\text{m}$ ]	Deviation .STL File
1	40,242	17.2	90.0	0.0286
2	1,994,398	19.5	101.2	0.0231
3	69,642	12.4	61.2	0.0258
4	40,242	17.9	87.4	0.0292
5	69,698	21.2	102.2	0.0331
6	1,994,398	18.4	90.9	0.0311
7	6114	17.8	82.2	0.0289
8	69,698	20.2	106.7	0.0314
9	11,304	20.4	95.1	0.0316
10	4880	20.6	109.3	0.0325
11	40,242	18.9	80.4	0.0318
12	1,994,398	15.2	79.3	0.0271
13	1,994,398	16.9	77.4	0.0282
14	10,502	14.6	88.3	0.0268
15	10,502	17.5	85.6	0.0285
16	4516	24.2	124.1	0.0347

**Table 4.** Surface roughness (Ra) at different layer thicknesses and scanning speeds [56].

Roughness, $\mu\text{m}$	Surface	30 $\mu\text{m}$	50 $\mu\text{m}$	70 $\mu\text{m}$
Scanning speed = 70 mm/s	Top	25.67	29.8	35.9
	Side	15.67	18.6	18.9
Scanning speed = 90 mm/s	Top	26	34	41.6
	Side	16.8	19.8	20

The interdependency of the surface quality and the laser process parameters, although it is mentioned in the literature, is still not yet fully analyzed or quantified. According

to Galy et al. [98], the usually adjusted parameters for surface improvement are those from energy input into the part contour. The surface variation often results from the adjustment of linear energy density consisting of laser power and scan speed, which is given by Equation (1). The  $\Psi$  is specific laser energy ( $\text{J}/\text{mm}^3$ ),  $P$  is the power of the laser (W),  $v$  is the scan speed of the laser ( $\text{mm}/\text{s}$ ),  $h$  is the inter-bead distance (mm) and  $d$  is the thickness of the layer of powder deposited (mm) [98].

$$\psi = \frac{P}{v \cdot h \cdot d} \quad (1)$$

However, as many researchers debate on the equation, the other parameters, such as laser spot diameter, the direction of gas flow and hatching strategies, are not deemed. This is due to the intensity of laser energy being varied by focal position via laser beam diameter on the build platform [92]. So, the interdependency of those parameters becomes a vital factor for the instability of melt pool size and shape and leads to balling, pores and variation on the up skin of the component. Chowdhury et al. [68] found that the tendency of ball formation can be reduced by increasing energy density. However, the excessive input energy causes the spreading and melting of the previous layer [46], which leads to another issue on the microstructure and forms complexity to other properties. In general, the common source of surface roughness can come from the powder, material and working chamber. However, the limited literature coverage is given for the factors from the chamber that includes the inert gas and limited oxygen. According to Li et al. [91], although shielding gas may prevent oxidization, it is very hard to completely eliminate the oxidation when the experiments were carried out in the air, especially for some active metals element.

### 5.3. Porosity of PBF-Produced Parts

One of the most common defects in SLM parts in general, irrespective of the material, is porosity, so more studies focus on the mechanism, causes and minimization of porosity [62,71,99–101]. According to Coro et al. [102], AM technology is an excellent choice for future designs. However, if the printing parameters are not fine-tuned, pores can emerge during the process. Due to the steep cooling rate process in the SLM, the cracking of parts is expected [101]. The presence of porosity potentially promotes cracking due to the notch effect [8,27,103–106]. Pores can develop over time due to entrained gas, chemical reactions, and supersaturated dissolved gases that create air holes in the melt pool [107]. The input process parameters responsible for the formation of porosity are suggested in the previous work of researchers. For instance, Peng et al. [101] developed the energy demand model to manufacture the SLM steel parts using critical parameters such as laser power, scan speed, layer thickness and hatch spacing.

The porosity in SLM can manifest on the surface or sub-surface. The sub-surface porosities are mostly located in the transitional zone between the counter path and the hatching path [8]. The porosity in the SLM is categorized into spherical (gas or hydrogen porosity) and irregular (keyhole or lack-of-fusion) morphology [27,72]. The size and shape of porosity indicate the phenomenon that has caused it [98]. The presence of moisture on the powder surface can easily capture hydrogen and contributes to the spherical morphology of pore development [62], which is known as metallurgical pores. In the other case, the presence of non-molten powder causes a lack of fusion, or keyhole pores are the categories under irregular morphology. According to Tang et al. [100], oxides formed during the melting and solidification of the sample are some of the conditions responsible for the formation of irregular morphology. This implies the parameters in the melting and solidification process contribute to the formation of irregular morphology porosities. The indirect description for porosity is the relative density of the part. Components that have lower relative density or higher pores are exposed to premature failure [107].

From the wing of laser parameters, most studies on reducing the rate of porosity within a material produced by SLM focus on the process and especially on the optimization

of the energy density factor. As mentioned earlier, energy density is the function of laser scan speed and laser power. Kimura et al. [107] investigated how energy density affects the development of pores. So, the finding suggests that the part's relative density dropped at both greater and lower energy densities. Incomplete melting of the powder causes porosity at lower energy densities, and at higher densities, many spherical porosities appear as morphological features of gas pores, either trapping argon from the combustion chamber due to the active flow of the molten metal or because the dissolved hydrogen aired during fusion. The relative density of A356.0 SLM specimens created with various levels of laser power at various scan speeds at a constant scan spacing of 0.1 mm is depicted in Figure 5a. The density of the specimens is reduced with increasing or decreasing scan speeds. For the specimens created at a specific scan speed and laser power setting, a peak density was discovered. The relative density of the specimens plotted as a function of scan spacing is shown in Figure 5b. In addition, the study conducted on Ti-6Al-4V fabricated by SLM indicates that as the interaction between high laser beam and powder particles at fixed layer thickness (20  $\mu\text{m}$ ), the samples contain low porosity when the speed is below 2700 mm/s [98]. Further increasing the speed led to an increase in porosity but not a significant one. Gong et al. [108] suggested the operator find optimum values to balance the parameters due to the result of his measured porosity showing increments of either too large or too small a beam spot size.

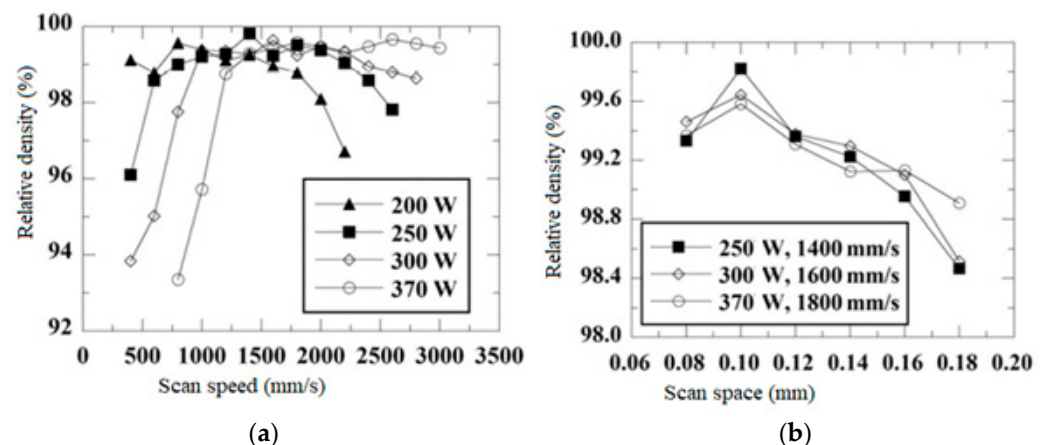


**Figure 5.** Relative density of SLM as (a). A function of scan speed and laser power, (b). Scan spacing. (Reused by permission from [107], License number 5464270902364).

In SLM, melting and solidification occur locally; the cooling rate is the function parameters such as beam power, beam speed, the pre-heat condition, build geometry and hatch spacing. Koutiri et al. [8] investigated the possible link between volume energy density and the porosity rate of SLM by incorporating the hatching distance with laser power and scanning speed. Two geometries of pores are observed as circular, which is close to the up skin and the irregular one, i.e., the keyhole with deeper beads formed around the overlap between the two strategies (contour and hatching). The dependence of porosity on those parameters is shown in Figure 6.

In the other case, higher relative density in powders improves the process by reducing internal stresses, part distortion and final part porosity [109]. This is due to the thermal conductivity increment with a relative density of the particle. The effects of powder particle size, shape and distribution on the porosity of the SLM part is another aspect. However, several researchers considered parameters related to energy density, such as laser power, scan speed, scan spacing and layer thickness [57,110,111]. The material absorptivity of laser energy and powder particle size needs to be considered to analyze the porosity formation rate.

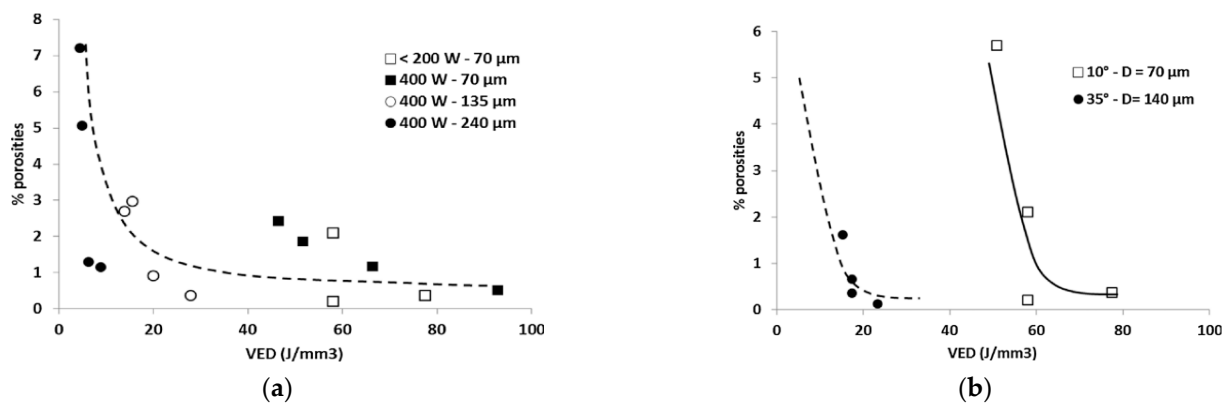


**Figure 6.** Dependence of porosity content versus process parameters in In625 for (a).  $P < 200$  W and  $P = 400$  W ( $10^\circ$ ), (b). Two distinct building angles ( $10^\circ$  and  $35^\circ$ ) (Adapted from [8] with permission, License number 5462380625001).

#### 5.4. Residual Stress in PBF-Produced Parts

High residual stresses are one of the fundamental phenomena that hinder SLM's widespread adoption in the industry, even though it is now a well-established metal manufacturing method. The stress is created by the large thermal gradients created by the laser that passes over an area with the powder rapidly melting, then back to solidification [18,49,62,112]. As the name suggests, these stresses remain in a component once the material has come to equilibrium with the environment [112,113]. Some of the effects of residual stresses are warping and thermal stress-related cracking, which cannot be corrected by post-processing [113]. Shrinkage is another form of shape distortion, which causes a lack of dimensional accuracy [112].

The exaggerated residual stress in SLM [62,112] inhibits the application of parts due to the aforementioned flaws. Therefore, it is crucial to identify input process parameter combinations that produce the smallest residual stress and associated defects magnitudes. The mechanism of residual stresses can be due to the temperature gradient that occurs at the laser spot and cooling rate. The mechanisms of residual stresses in SLM are well explained in [112]. The major defects due to residual stresses are dimensional deviation [114], delamination, stress-induced cracking and accelerated crack growth, which leads to early fatigue failure [115]. Warping, distortions and cracking are irreversible by post-processing techniques such as stress relief heat treatment [116,117]. Therefore, due to the catastrophic failure of components, understanding the process parameters responsible for the cause of residual stress is crucial for mitigation in advance. The negative impacts of residual stresses can be greatly diminished by manipulating one or more of the process parameters. As mentioned by Mugwagwa et al. [115], some of the factors that influence residual stresses include scanning patterns, scan vector lengths, scan vector angles, rotation angles between layers, part geometry, material type, support types and pre-heating conditions. The residual stress formation and process parameter mapping of SLM needs deep insight and still require more consideration.

Several authors identified influential process parameters responsible for the induced residual stress. For instance, Yadroitsev et al. [117] considered laser power, layer thickness and scanning speed to analyze the residual stress of SLM, while several researchers considered laser power and scanning speed [118–120]. The effect of process gas, scan speed and sample thickness on the buildup residual stresses and porosity in Ti-6Al-4V produced by SLM was studied [121]. In the other case, the common defect in SLM porosity has a positive effect on the residual stress [115,122,123]. That is the trick that needs to be emphasized in the research to clarify at what level of porosity is tolerated to handle the residual stress without exposing the components because of the porosity. The scatter plot in Figure 7 shows that pores indeed have the effect of relaxing residual stresses, and higher porosity leads to less distortion. The interdependence of porosity and residual stress will

give consideration to both influential process parameters. In several studies, the constraints from powder particles and individual influential process parameters for distortion, residual stress and porosity are not clearly considered, and the focus of the studies was to reveal the relationship among the responses.

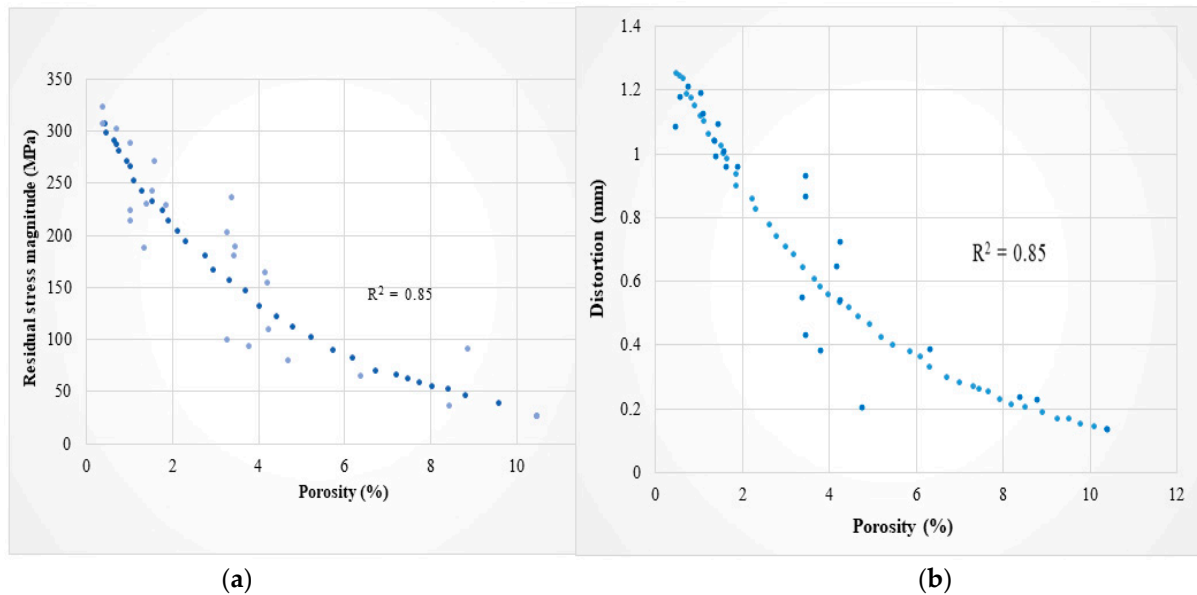


**Figure 7.** SLM interdependencies: (a) Porosity residual stresses, (b) Porosity distortions (Adapted from [115] with permission in accordance with Creative Common CC BY license, open access).

The influence of energy density on the residual stress is studied. When parameters are varied simultaneously, there is no observable influence of energy density on residual stresses, as shown in Figure 8. Thus, according to Mugwagwa et al. [115], energy density cannot be used to explain or account for the differences in the observed process outcome, which is similar to the observation of Prashanth [58]. However, the energy density is the function of laser power and scanning speed; considering those parameters, one factor may affect the result.

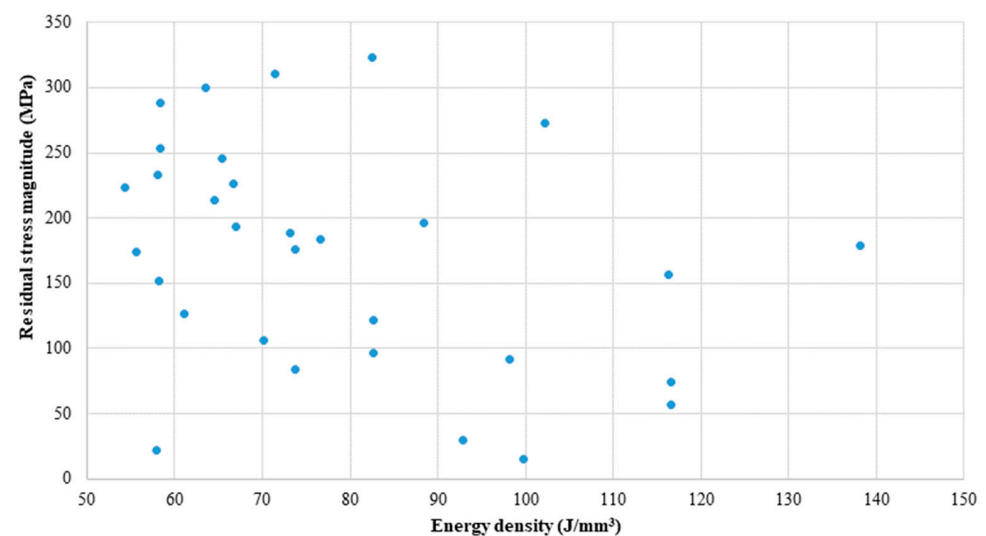


**Figure 8.** Scatter plots of the effect of energy density on residual stress magnitude (Adapted from [115] with permission in accordance with Creative Common CC BY license, open access).

### 5.5. Repeatability and Reproducibility Issues of PBF Process

According to the review article published in 2014 by Tapia et al. [6], a consensus among experts and stakeholders in the aerospace, healthcare and automotive fields indicate that metallic AM parts are still not sufficient to meet their strict requirements. The high-tech industries demand overall equipment effectiveness (OEE), which must be better than 70%, with scrap rates of less than 1000 ppm as a crucial criterion. The current world-class vehicle manufacturer's OEE is increased to 85% [49]. Weller et al. [124] further demonstrated the consensus in a comprehensive economic review on the implications and limitations of AM in the industry, and the greatest barrier is identified as the limitation of repeatability and reproducibility of parts, which affects the OEE calculations. According to ASTM E117, repeatability is precision under the conditions where independent test results are obtained with the same method on identical test items in the same laboratory by the same operator using the same equipment within short intervals of time [49]. Reproducibility is similar, but the test can be carried out in different laboratories, with different operators and using different equipment. The high volume of research has focused on the capability of AM, but there is a lack of research coverage focused on its repeatability and reproducibility.

The product quality and reliability characteristics, i.e., dimensional accuracy, precision, repeatability and reproducibility, are mostly affected by inherent and systematic manufacturing process variations [18]. One of the common errors that occur in PBF is dimensional accuracy. Researchers focused on the source of variation in the geometry and mechanical properties of parts. For instance, Franchitti et al. [125] considered orientation angle, build location and build height effects on the dimensional accuracy of Ti-6Al-4V rectangular parts fabricated by the EBM process. Thus, sample orientation and build location were identified as the influential source of dimensional variations. The mechanical precision of the manufacturing setup, such as layer thickness, concentrated laser spot size and scanner's position precision, is among the factors affecting dimensional accuracy [18]. According to Abedi et al. [126] The process variables such as temperature, strain and strain rate have a direct impact on the suggested constitutive equations' precision and repeatability. Calignano et al. [97] investigated the dimensional accuracy of L-PBF using AlSi10Mg alloy and stated that the accuracy of parts produced is affected by the .STL file, build direction and process parameters. The choice of parameters for the .STL file affects not only the accuracy but also the surface roughness of the part's build direction [96] and other process parameters [18]. Here, dimensional repeatability is considered, and the mechanical property of the part is not covered, and that is the unseen part of the literature. However, researchers investigated the repeatability and reproducibility of PBF through the statistical analysis of standard deviation, where each data set represents different operating parameters. This conflicts with the definition given by ASTM E117.

The issue of repeatability and reproducibility needs the various aspects, powder particles, laser parameters, materials and the printing chamber environments. According to Dawes et al. [55], the more different the PSD in cobalt chrome, the better the ultimate tensile strength obtained as the size of the powder increases; however, the repeatability of these parts is reduced. This implies the PSD has contributed to altering the repeatability of the part. The flowability of the powder has direct effects on the supplied layer thickness of parts and yields different yield strengths and UTS [49].

In the other case, the consequence of other defects like residual stress can have effects on the repeatability of the part. The volume shrinkage and thermal gradients together lead to warpage and distortion, which causes dimensional inaccuracies and loss of quality in the final part [96]. The effects of stair-stepping due to the layered nature of part construction which is heavily dependent on part orientation [94], in addition to surface roughness, can cause dimensional inaccuracies.

## 6. Conclusions

In this article, a review of the recent literature on research advances and applications of powder-bed fusion-based additive manufacturing technology is conducted. The study

focused on SLM-based AM technology, and based on the review, the following conclusions are observed.

- In general, the current status of the SLM production process indicates that it is still expensive and slow compared to the conventional manufacturing process. The components are typically semi-finished and need post-processing.
- PBF-based metal AM received attention from R&D due to its rewards, such as a high degree of product customization and minimum buy-to-fly ratio. Moreover, the SLM has the capacity to manufacture materials that would be difficult by other manufacturing processes.
- The comparison of PBF and its sub-categories with other related processes, such as DED, are among the concerns of the industries. The status of PBF indicates that SLM is an emerging candidate for mission-oriented applications like aerospace, defense and healthcare, while EB-PBF is a newer and less explored technology with limited applications.
- SLM suffers from the drawbacks such as reliability and quality in terms of dimensional accuracy, strength and surface roughness.
- The outcome of SLM largely depends on process parameters and the interplay of physical phenomena. As the status and demand of SLM are changing from a rapid prototype to mass production and then to customized production, the underdeveloped issues related to processing parameters are a great future concern of the research for the competence of the technology.
- Mapping process parameters with the outcome is the safest alternative to finding the root cause of variations and monitoring in advance. However, the involved process parameters in the phenomena are complex and change in a timescale. Controlling certain quality aspects of a part could highly affect the unseen aspects. This paper grouped the source of process parameters to powder morphology-related laser parameters, feedstock material properties and printing chamber environments. The finding is a vital input for the bottom-up approach. In addition, considering the relationships of the involved process parameters will lead to fruitful results on the quality of the components.

**Author Contributions:** Conceptualization, N.D.D. and H.G.L.; methodology, N.D.D.; software, N.D.D.; validation, H.G.L.; formal analysis, N.D.D.; investigation, N.D.D.; resources, H.G.L.; data curation, N.D.D.; writing—original draft preparation, N.D.D.; writing—review and editing, H.G.L.; visualization, N.D.D. and H.G.L.; supervision, H.G.L.; project administration, H.G.L.; funding acquisition, H.G.L. All authors have read and agreed to the published version of the manuscript.

**Funding:** This research was supported by the INDMET project, grant number 62862, funded by the NORHED II program.

**Institutional Review Board Statement:** Not applicable.

**Data Availability Statement:** Not applicable.

**Conflicts of Interest:** The authors declare no conflict of interest.

## References

1. Colosimo, B.M.; Huang, Q.; Dasgupta, T.; Tsung, F. Opportunities and challenges of quality engineering for additive manufacturing. *J. Qual. Technol.* **2018**, *50*, 233–252. [[CrossRef](#)]
2. Mehrpouya, M.; Tuma, D.; Vaneker, T.; Afrasiabi, M.; Bambach, M.; Gibson, I. Multi-material powder bed fusion techniques. *Rapid Prototyp. J.* **2022**, *28*, 1–19. [[CrossRef](#)]
3. Dilberoglu, U.M.; Gharehpapagh, B.; Yaman, U.; Dolen, M. The Role of Additive Manufacturing in the Era of Industry 4.0. *Procedia Manuf.* **2017**, *11*, 545–554. [[CrossRef](#)]
4. Dovggy, B. Assessing the Printability of Alloys in Fusion-Based Additive Manufacturing: Towards Criteria for Alloy Selection. Doctoral Dissertation, Imperial College: London, UK, 2022.
5. Lewis, G. Aspects of the Powder in Metal Additive Manufacturing: Review. *World J. Text. Eng. Technol.* **2022**, *10*, 363–409. [[CrossRef](#)]

6. Tapia, G.; Elwany, A. A review on process monitoring and control in metal-based additive manufacturing. *J. Eng. Ind.* **2014**, *136*, 60801. [[CrossRef](#)]
7. Babuska, T.F.; Krick, B.A.; Susan, D.F.; Kustas, A.B. Comparison of powder bed fusion and directed energy deposition for tailoring mechanical properties of traditionally brittle alloys. *Manuf. Lett.* **2021**, *28*, 30–34. [[CrossRef](#)]
8. Koutiri, I.; Pessard, E.; Peyre, P.; Amlou, O.; De, T.T. Influence of SLM process parameters on the surface finish, porosity rate and fatigue behavior of as-built Inconel 625 parts. *J. Mater. Process. Technol.* **2018**, *255*, 536–546. [[CrossRef](#)]
9. Chen, Z.; Han, C.; Gao, M.; Kandukuri, S.Y.; Zhou, K. A review on qualification and certification for metal additive manufacturing. *Virtual Phys. Prototyp.* **2022**, *17*, 382–405. [[CrossRef](#)]
10. Wohlers, T.; Gornet, T. History of additive manufacturing. *Wohlers Rep.* **2014**, *24*, 118.
11. Lee, J.Y.; An, J.; Chua, C.K. Fundamentals, and applications of 3D printing for novel materials. *Appl. Mater. Today* **2017**, *7*, 120–133. [[CrossRef](#)]
12. Gibson, I.; Rosen, D.; Stucker, B.; Khorasani, M. Design for additive manufacturing. In *Additive Manufacturing Technologies*; Springer: Cham, Switzerland, 2021; pp. 555–607.
13. Singh, R.; Gupta, A.; Tripathi, O.; Srivastava, S.; Singh, B.; Awasthi, A.; Rajput, S.K.; Sonia, P.; Singhal, P.; Saxena, K.K. Powder bed fusion process in additive manufacturing: An overview. *Mater. Today Proc.* **2020**, *26*, 3058–3070. [[CrossRef](#)]
14. Garcia-Colomo, A.; Wood, D.; Martina, F.; Williams, S.W. A comparison framework to support the selection of the best additive manufacturing process for specific aerospace applications. *Int. J. Rapid Manuf.* **2020**, *9*, 194–211. [[CrossRef](#)]
15. Ladani, L.; Sadeghilaridjani, M. Review of powder bed fusion additive manufacturing for metals. *Metals* **2021**, *11*, 1391. [[CrossRef](#)]
16. Murugan, P.D.; Vijayananth, S.; Natarajan, M.P.; Jayabalakrishnan, D.; Arul, K.; Jayaseelan, V.; Elanchezian, J. A current state of metal additive manufacturing methods: A review. *Mater. Today Proc.* **2021**, *59*, 1277–1283. [[CrossRef](#)]
17. Martin, J.M.; Yahata, B.D.; Hundley, J.M.; Mayer, J.A.; Schaedler, T.A.; Pollock, T.M. 3D printing of high-strength aluminum alloys. *Nature* **2017**, *549*, 365–369. [[CrossRef](#)]
18. Ahmed, A.; Majeed, A.; Atta, Z.; Jia, G. Dimensional quality, and distortion analysis of thin-walled alloy parts of AlSi10Mg manufactured by selective laser melting. *J. Manuf. Mater. Process.* **2019**, *3*, 51. [[CrossRef](#)]
19. Gibson, I.; Rosen, D.; Stucker, B.; Khorasani, M. *Additive Manufacturing Technologies*, 3rd ed.; Springer: Cham, Switzerland, 2021; Volume 17.
20. Džugan, J.; Nový, Z. *Powder Application in Additive Manufacturing of Metallic Parts. Powder Metallurgy: Fundamentals and Case Studies*; InTechOpen: Rijeka, Croatia, 2017; p. 183.
21. Ahmadi, M.; Tabary, B.; Rahmatabadi, D.; Ebrahimi, S.; Abrinia, K.; Hashemi, R. Review of selective laser melting of magnesium alloys: Advantages, microstructure and mechanical characterizations, defects, challenges, and applications. *J. Mater. Res. Technol.* **2022**, *19*, 1537–1562. [[CrossRef](#)]
22. Yang, L.; Hsu, K.; Baughman, B.; Godfrey, D.; Medina, F.; Menon, M.; Wiener, S. *Additive Manufacturing of Metals: The Technology, Materials, Design, and Production*; Springer: Cham, Switzerland, 2017; pp. 45–61.
23. Vafadar, A.; Guzzomi, F.; Rassau, A.; Hayward, K. Advances in metal additive manufacturing: A review of common processes, industrial applications, and current challenges. *Appl. Sci.* **2021**, *11*, 1213. [[CrossRef](#)]
24. Korpela, M.; Riikonen, N.; Piili, H.; Salminen, A.; Nyrhilä, O. Additive manufacturing—Past, present, and the future. In *Technical, Economic, and Societal Effects of Manufacturing 4.0*; Palgrave Macmillan: Cham, Switzerland, 2020; pp. 17–41.
25. King, W.E.; Anderson, A.T.; Ferencz, R.M.; Hodge, N.E.; Kamath, C.; Khairallah, S.A.; Rubenchik, A.M. Laser powder bed fusion additive manufacturing of metals; physics, computational, and materials challenges. *Appl. Phys. Rev.* **2015**, *2*, 041304. [[CrossRef](#)]
26. Wang, Y.; Chen, X.; Jayalakshmi, S.; Singh, R.A.; Sergej, K.; Gupta, M. Process parameters, product quality monitoring, and control of powder bed fusion. In *Transactions on Intelligent Welding Manufacturing*; Springer: Singapore, 2020; pp. 89–108.
27. Maurya, A.K.; Kumar, A. Defect and Distortion in Powder Bed Fusion of Metal Additive Manufacturing Parts. *ASEAN J. Sci. Technol. Dev.* **2022**, *39*, 85–103. [[CrossRef](#)]
28. Milewski, J.O. *Additive Manufacturing of Metals*; Springer International Publishing AG: Cham, Switzerland, 2017; Volume 258, pp. 134–1577.
29. Chua, Z.Y.; Ahn, I.H.; Moon, S.K. Process monitoring and inspection systems in metal additive manufacturing: Status and applications. *Int. J. Precis. Eng. Manuf.-Green Tech.* **2017**, *4*, 235–245. [[CrossRef](#)]
30. Childerhouse, T.; Jackson, M. Near net shape manufacture of titanium alloy components from powder and wire: A review of state-of-the-art process routes. *Metals* **2019**, *9*, 689. [[CrossRef](#)]
31. Dutta, B.; Froes, F.S. The additive manufacturing of titanium alloys. *Met. Powder Rep.* **2017**, *72*, 96–106.
32. Pal, R.; Basak, A. Linking Powder Properties, Printing Parameters, Post-Processing Methods, and Fatigue Properties in Additive Manufacturing of AlSi10Mg. *Alloys* **2022**, *1*, 149–179. [[CrossRef](#)]
33. Francis, Z.R. The Effects of Laser and Electron Beam Spot Size in Additive Manufacturing Processes. Doctoral Dissertation, Carnegie Mellon University, Pittsburgh, PA, USA, 2017.
34. Baumers, M.; Dickens, P.; Tuck, C.; Hague, R. The cost of additive manufacturing: Machine productivity, economies of scale and technology-push. *Technol. Forecast. Soc. Chang.* **2016**, *102*, 193–201. [[CrossRef](#)]
35. Sames, W. Additive Manufacturing of Inconel 718 Using Electron Beam Melting: Processing, Post-Processing, & Mechanical Properties. Doctoral Dissertation, Texas A & M University, College Station, TX, USA, 2015.

36. Ding, D.; Pan, Z.; Cuiuri, D.; Li, H. Wire-feed additive manufacturing of metal components: Technologies, developments, and future interests. *Int. J. Adv. Manuf. Technol.* **2015**, *81*, 465–481.
37. Vayre, B.; Vignat, F.; Villeneuve, F. Metallic additive manufacturing: State-of-the-art review and prospects. *Mech. Ind.* **2012**, *13*, 89–96. [[CrossRef](#)]
38. Boley, C.D.; Khairallah, S.A.; Rubenchik, A.M. Calculation of laser absorption by metal powders in additive manufacturing. In *Additive Manufacturing Handbook*; CRC Press: Boca Raton, FL, USA, 2017; pp. 507–509.
39. Gu, D. *Laser Additive Manufacturing (AM): Classification, Processing Philosophy, and Metallurgical Mechanisms*; Springer: Berlin/Heidelberg, Germany, 2015; pp. 15–71.
40. Popov, V.V.; Grilli, M.L.; Koptuyg, A.; Jaworska, L.; Katz-Demyanetz, A.; Klobčar, D.; Balos, S.; Postolnyi, B.O.; Goel, S. Powder bed fusion additive manufacturing using critical raw materials: A review. *Materials* **2021**, *14*, 909. [[CrossRef](#)]
41. Oliveira, J.P.; Lalonde, A.D.; Ma, J. Processing parameters in laser powder bed fusion metal additive manufacturing. *Mater. Des.* **2020**, *193*, 1–12. [[CrossRef](#)]
42. Sow, M.C.; De, T.T.; Castelnaud, O.; Hamouche, Z.; Coste, F.; Fabbro, R.; Peyre, P. Influence of beam diameter on Laser Powder Bed Fusion (L-PBF) process. *Addit. Manuf.* **2020**, *36*, 101532.
43. Narasimharaju, S.R.; Zeng, W.; See, T.L.; Zhu, Z.; Scott, P.; Jiang, X.; Lou, S. A comprehensive review on laser powder bed fusion of steels: Processing, microstructure, defects and control methods, mechanical properties, current challenges, and future trends. *J. Manuf. Process.* **2022**, *75*, 375–414. [[CrossRef](#)]
44. Montazeri, M.; Rao, P. Sensor-based build condition monitoring in laser powder bed fusion additive manufacturing process using a spectral graph theoretic approach. *J. Manuf. Sci. Eng.* **2018**, *140*, 091002-1. [[CrossRef](#)]
45. Zhang, B.; Li, Y.; Bai, Q. Defect Formation Mechanisms in Selective Laser Melting. A Review. *Chin. J. Mech. Eng.* **2017**, *30*, 515–527. [[CrossRef](#)]
46. Javidrad, H.R.; Salemi, S. Effect of the volume energy density and heat treatment on the defect, microstructure, and hardness of L-PBF Inconel 625. *Metall. Mater. Trans A* **2020**, *51*, 5880–5891. [[CrossRef](#)]
47. Klingbeil, N.W.; Beuth, J.L.; Chin, R.K.; Amon, C.H. Residual stress-induced warping in direct metal solid freeform fabrication. *Int. J. Mech. Sci.* **2002**, *44*, 57–77. [[CrossRef](#)]
48. Kladovasilakis, N.; Charalampous, P.; Kostavelis, I.; Tzetzis, D.; Tzovaras, D. Impact of metal additive manufacturing parameters on the powder bed fusion and direct energy deposition processes: A comprehensive review. *Prog. Addit. Manuf.* **2021**, *6*, 349–365. [[CrossRef](#)]
49. Dowling, L.; Kennedy, J.; O’Shaughnessy, S.; Trimble, D. A review of critical repeatability and reproducibility issues in powder bed fusion. *Mater. Des.* **2020**, *186*, 108346. [[CrossRef](#)]
50. Scime, L.; Beuth, J. Anomaly detection and classification in a laser powder bed additive manufacturing process using a trained computer vision algorithm. *Addit. Manuf.* **2018**, *19*, 114–126. [[CrossRef](#)]
51. Kulkarni, P.A.; Berry, R.J.; Bradley, M.S. Review of the flowability measuring techniques for powder metallurgy industry. Proceedings of the Institution of Mechanical Engineers. *J. Process Mech. Eng. Part E* **2010**, *224*, 159–168. [[CrossRef](#)]
52. Karapatis, N.P.; Egger, G.; Gygas, P.E.; Glardon, R. Optimization of powder layer density in selective laser sintering. In *1999 International Solid Freeform Fabrication Symposium*; The University of Texas at Austin: Austin, TX, USA, 1999. [[CrossRef](#)]
53. Slotwinski, J.A.; Garboczi, E.J.; Stutzman, P.E.; Ferraris, C.F.; Watson, S.S.; Peltz, M.A. Characterization of metal powders used for additive manufacturing. *J. Res. Natl. Inst. Stand. Technol.* **2014**, *119*, 460. [[CrossRef](#)]
54. Yuan, B.; Guss, G.M.; Wilson, A.C.; Hau-Riege, S.P.; DePond, P.J.; McMains, S.; Matthews, M.J.; Giera, B. Machine-learning-based monitoring of laser powder bed fusion. *Adv. Mater. Technol.* **2018**, *3*, 1800136. [[CrossRef](#)]
55. Dawes, J.; Bowerman, R.; Trepleton, R. Introduction to the Additive Manufacturing Powder Metallurgy Supply Chain Exploring the production and supply of metal powders for AM processes. *Johns. Matthey Technol. Rev.* **2015**, *3*, 243–256. [[CrossRef](#)]
56. Spierings, A.B.; Herres, N.; Levy, G. Influence of the particle size distribution on surface quality and mechanical properties in AM steel parts. *Rapid Prototyp. J.* **2011**, *17*, 195–202. [[CrossRef](#)]
57. Cherry, J.A.; Davies, H.M.; Mehmood, S.; Lavery, N.P.; Brown, S.G.; Sienz, J. Investigation into the effect of process parameters on microstructural and physical properties of 316L stainless steel parts by selective laser melting. *Int. J. Adv. Manuf. Technol.* **2015**, *76*, 869–879. [[CrossRef](#)]
58. Attar, H.; Prashanth, K.G.; Zhang, L.C.; Calin, M.; Okulov, I.V.; Scudino, S.; Yang, C.; Eckert, J. Effect of powder particle shape on the properties of in situ Ti–TiB composite materials produced by selective laser melting. *J. Mater. Sci. Technol.* **2015**, *31*, 1001–1005. [[CrossRef](#)]
59. Polozov, I.; Sufiiarov, V.; Kantyukov, A.; Razumov, N.; Goncharov, I.; Makhmutov, T.; Silin, A.; Kim, A.; Starikov, K.; Shamshurin, A.; et al. Microstructure, densification, and mechanical properties of titanium intermetallic alloy manufactured by laser powder bed fusion additive manufacturing with high-temperature preheating using gas atomized and mechanically alloyed plasma spheroidized powders. *Addit. Manuf.* **2020**, *34*, 101374. [[CrossRef](#)]
60. Sanaei, D. Characteristics and analysis of their variability in metal L-PBF additive manufacturing. *Mater. Des.* **2019**, *182*, 108091. [[CrossRef](#)]
61. Ardila, L.C.; Garcíandia, F.; González-Díaz, J.B.; Álvarez, P.; Echeverría, A.; Petite, M.M.; Deffley, R.; Ochoa, J. Effect of IN718 recycled powder reuse on properties of parts manufactured by means of selective laser melting. *Phys. Procedia* **2014**, *56*, 99–107. [[CrossRef](#)]

62. Aboulkhair, N.T.; Simonelli, M.; Parry, L.; Ashcroft, I.; Tuck, C.; Hague, R. 3D printing of Aluminium alloys: Additive Manufacturing of Aluminum alloys using selective laser melting. *Prog. Mater. Sci.* **2019**, *106*, 100578. [[CrossRef](#)]
63. Simonelli, M.; Tuck, C.; Aboulkhair, N.T.; Maskery, I.; Ashcroft, I.; Wildman, R.D.; Hague, R. A study on the laser spatter and the oxidation reactions during selective laser melting of 316L stainless steel, Al-Si10-Mg, and Ti-6Al-4V. *Metall. Mater. Trans. A* **2015**, *46*, 3842–3851. [[CrossRef](#)]
64. Maamoun, A.H.; Elbestawi, M.; Dosbaeva, G.K.; Veldhuis, S.C. Thermal post-processing of AlSi10Mg parts produced by Selective Laser Melting using recycled powder. *Addit. Manuf.* **2018**, *21*, 234–247. [[CrossRef](#)]
65. Kamath, C. Data mining and statistical inference in selective laser melting. *Int. J. Adv. Manuf. Technol.* **2016**, *86*, 1659–1677. [[CrossRef](#)]
66. Berumen, S.; Bechmann, F.; Lindner, S.; Kruth, J.P.; Craeghs, T. Quality control of laser-and powder bed-based Additive Manufacturing (AM) technologies. *Phys. Procedia* **2010**, *5*, 617–622. [[CrossRef](#)]
67. Verhaeghe, G.; Hilton, P. The effect of spot size and laser beam quality on welding performance when using high-power continuous wave solid-state lasers. *Int. Congr. Appl. Lasers Electro-Op. Laser Instit. Am.* **2005**, *2005*, 507.
68. Chowdhury, S.; Yadaiah, N.; Prakash, C.; Ramakrishna, S.; Dixit, S.; Gulta, L.R.; Buddhi, D. Laser powder bed fusion: A state-of-the-art review of the technology, materials, properties & defects, and numerical modeling. *J. Mater. Res. Technol.* **2022**, *20*, 2109–2172.
69. Mudge, R.P.; Wald, N.R. Laser-engineered net shaping advances additive manufacturing and repair. *Weld. J.-N. Y.* **2007**, *86*, 44.
70. Bi, G.; Sun, C.N.; Gasser, A. Study on influential factors for process monitoring and control in laser aided additive manufacturing. *J. Mater. Process. Technol.* **2013**, *213*, 463–468. [[CrossRef](#)]
71. Aboulkhair, N.T.; Everitt, N.M.; Ashcroft, I.; Tuck, C. Reducing porosity in AlSi10Mg parts processed by selective laser melting. *Addit. Manuf.* **2014**, *1*, 77–86. [[CrossRef](#)]
72. Chia, H.Y.; Wu, J.; Wang, X.; Yan, W. Process parameter optimization of metal additive manufacturing: A review and outlook. *J. Mater. Inf.* **2022**, *2*, 16. [[CrossRef](#)]
73. Wu, J.; Wang, X.Q.; Wang, W.; Attallah, M.M.; Loretto, M.H. Microstructure and strength of selective laser melted AlSi10Mg. *Acta Mater.* **2016**, *117*, 311–320. [[CrossRef](#)]
74. Siddique, S.; Imran, M.; Wycisk, E.; Emmelmann, C.; Walther, F. Influence of process-induced microstructure and imperfections on mechanical properties of AlSi12 processed by selective laser melting. *J. Mater. Process. Technol.* **2015**, *221*, 205–213. [[CrossRef](#)]
75. Shi, X.; Ma, S.; Liu, C.; Wu, Q.; Lu, J.; Liu, Y. Materials Science & Engineering A Selective laser melting-wire arc additive manufacturing hybrid fabrication of Ti-6Al-4V alloy: Microstructure and mechanical properties. *Mater. Sci. Eng. A* **2017**, *684*, 196–204.
76. Pérez-Ruiz, J.D.; de Lacalle, L.N.L.; Urbikain, G.; Pereira, O.; Martínez, S.; Bris, J. On the relationship between cutting forces and anisotropy features in the milling of LPBF Inconel 718 for near net shape parts. *Int. J. Mach. Tools Manuf.* **2021**, *170*, 103801. [[CrossRef](#)]
77. Pérez-Ruiz, J.D.; Martín, F.; Martínez, S.; Lamikiz, A.; Urbikain, G.; López de Lacalle, L.N. Stiffening near-net-shape functional parts of Inconel 718 LPBF considering material anisotropy and subsequent machining issues. *Mech. Syst. Process.* **2022**, *168*, 108675. [[CrossRef](#)]
78. Trelewicz, J.R.; Halada, G.P.; Donaldson, O.K.; Manogharan, G. Microstructure and corrosion resistance of laser additively manufactured 316L stainless steel. *JOM* **2016**, *68*, 850–859. [[CrossRef](#)]
79. Wen, X.; Wan, M.; Huang, C.; Tan, Y.; Lei, M.; Liang, Y.; Cai, X. Effect of microstructure on tensile properties, impact toughness and fracture toughness of TC21 alloy. *Mater. Des.* **2019**, *180*, 107898. [[CrossRef](#)]
80. Toribio, J.; González, B.; Matos, J.C.; Ayaso, F.J. Influence of microstructure on strength and ductility in fully pearlitic steels. *Metals* **2016**, *6*, 318. [[CrossRef](#)]
81. Yang, P.; Deibler, L.A.; Bradley, D.R.; Stefan, D.K.; Carroll, J.D. Microstructure evolution and thermal properties of an additively manufactured, solution treatable AlSi10Mg part. *J. Mater. Res.* **2018**, *33*, 4040–4052. [[CrossRef](#)]
82. Koike, M.; Greer, P.; Owen, K.; Lilly, G.; Murr, L.E.; Gaytan, S.M.; Martínez, E.; Okabe, T. Evaluation of titanium alloys fabricated using rapid prototyping technologies electron beam melting and laser beam melting. *Materials* **2011**, *4*, 1776–1792. [[CrossRef](#)]
83. Hibino, S.; Todo, T.; Ishimoto, T.; Gokcekaya, O.; Koizumi, Y.; Igashira, K.; Nakano, T. Control of crystallographic texture and mechanical properties of Hastelloy-X via laser powder bed fusion. *Crystals* **2021**, *11*, 1064. [[CrossRef](#)]
84. Ishimoto, T.; Nakano, T. Microstructural Control and Functional Enhancement of Light Metal Materials via Metal Additive Manufacturing. *Mater. Trans.* **2023**, *64*, 10–16. [[CrossRef](#)]
85. Todo, T.; Ishimoto, T.; Gokcekaya, O.; Oh, J.; Nakano, T. Single crystalline-like crystallographic texture formation of pure tungsten through laser powder bed fusion. *Scr. Mater.* **2022**, *206*, 114252. [[CrossRef](#)]
86. Niendorf, T.; Leuders, S.; Riemer, A.; Richard, H.A.; Tröster, T.; Schwarze, D. Highly anisotropic steel processed by selective laser melting. *Metall. Mater. Trans. B* **2013**, *44*, 794–796. [[CrossRef](#)]
87. Nguyen, Q.B.; Luu, D.N.; Nai, S.M.; Zhu, Z.; Chen, Z.; Wei, J. The role of powder layer thickness on the quality of SLM printed parts. *Arch. Civ. Mech. Eng.* **2018**, *18*, 948–955. [[CrossRef](#)]
88. Li, J.; Ren, H.; Liu, C.; Shang, S. The effect of specific energy density on microstructure and corrosion resistance of CoCrMo alloy fabricated by laser metal deposition. *Materials* **2019**, *12*, 1321. [[CrossRef](#)]

89. Ge, W.; Guo, C.; Lin, F. Effect of process parameters on microstructure of TiAl alloy produced by electron beam selective melting. *Procedia Eng.* **2014**, *81*, 1192–1197. [[CrossRef](#)]
90. Calleja-Ochoa, A.; Gonzalez-Barrio, H.; López de Lacalle, N.; Martínez, S.; Albizuri, J.; Lamikiz, A. A new approach in the design of microstructured ultralight components to achieve maximum functional performance. *Materials* **2021**, *14*, 1588. [[CrossRef](#)]
91. Li, Y.; Yang, H.; Lin, X.; Huang, W.; Li, J.; Zhou, Y. The influences of processing parameters on forming characterizations during laser rapid forming. *Mater. Sci. Eng. A* **2003**, *360*, 18–25. [[CrossRef](#)]
92. Rott, S.; Ladewig, A.; Friedberger, K.; Casper, J.; Full, M.; Schleifenbaum, J.H. Surface roughness in laser powder bed fusion—Interdependency of surface orientation and laser incidence. *Addit. Manuf.* **2020**, *36*, 101437. [[CrossRef](#)]
93. Spierings, A.B.; Voegtlin, M.; Bauer, T.U.; Wegener, K. Powder flowability characterization methodology for powder-bed-based metal additive manufacturing. *Progress Addit. Manuf.* **2016**, *1*, 9–20. [[CrossRef](#)]
94. Abd-Elghany, K.; Bourell, D.L. Property evaluation of 304L stainless steel fabricated by selective laser melting. *Rapid Prototyp. J.* **2012**, *18*, 420–428. [[CrossRef](#)]
95. Delfs, P.; Tows, M.; Schmid, H.J. Optimized build orientation of additive manufactured parts for improved surface quality and build time. *Addit. Manuf.* **2016**, *12*, 314–320. [[CrossRef](#)]
96. Di Angelo, L.; Di Stefano, P.; Guardiani, E. Search for the optimal build direction in additive manufacturing technologies: A review. *J. Manuf. Mater. Process.* **2020**, *4*, 71. [[CrossRef](#)]
97. Calignano, F.; Lorusso, M.; Pakkanen, J.; Trevisan, F.; Ambrosio, E.P.; Manfredi, D.; Fino, P. Investigation of accuracy and dimensional limits of part produced in aluminum alloy by selective laser melting. *Int. J. Adv. Manuf. Technol.* **2017**, *88*, 451–458. [[CrossRef](#)]
98. Galy, C.; Le Guen, E.; Lacoste, E.; Arvieu, C. Main defects observed in aluminum alloy parts produced by SLM: From causes to consequences. *Addit. Manuf.* **2018**, *22*, 165–175. [[CrossRef](#)]
99. Qiu, C.; Panwisawas, C.; Ward, M.; Basoalto, H.C.; Brooks, J.W.; Attallah, M.M. On the role of melt flow into the surface structure and porosity development during selective laser melting. *Acta Mater.* **2015**, *96*, 72–79. [[CrossRef](#)]
100. Tang, M.; Pistorius, P.C. Oxides, porosity, and fatigue performance of AlSi10Mg parts produced by selective laser melting. *Int. J. Fatigue* **2017**, *94*, 192–201. [[CrossRef](#)]
101. Peng, T.; Chen, C. Influence of energy density on energy demand and porosity of 316L stainless steel fabricated by selective laser melting. *Int. J. Precis. Eng. Manuf.-Green Tech.* **2018**, *5*, 55–62. [[CrossRef](#)]
102. Coro, A.; Macareno, L.M.; Aguirrebeitia, J.; López de Lacalle, N. A methodology to evaluate the reliability impact of the replacement of welded components by additive manufacturing spare parts. *Metals* **2019**, *9*, 932. [[CrossRef](#)]
103. Wei, C.; Li, L. Recent progress and scientific challenges in multi-material additive manufacturing via laser-based powder bed fusion. *Virtual Phys. Prototyp.* **2021**, *16*, 347–371. [[CrossRef](#)]
104. Kaufmann, N.; Imran, M.; Wischeropp, T.M.; Emmelmann, C.; Siddique, S.; Walther, F. Influence of process parameters on the quality of aluminum alloy EN AW 7075 using selective laser melting (SLM). *Phys. Procedia* **2016**, *83*, 918–926. [[CrossRef](#)]
105. Sames, W.J.; List, F.A.; Pannala, S.; Dehoff, R.R.; Babu, S.S. The metallurgy and processing science of metal additive manufacturing. *Int. Mater. Rev.* **2016**, *61*, 315–360. [[CrossRef](#)]
106. Parthasarathy, J.; Starly, B.; Raman, S.; Christensen, A. Mechanical evaluation of porous titanium (Ti6Al4V) structures with electron beam melting (EBM). *J. Mech. Behav. Biomed. Mater.* **2010**, *3*, 249–259. [[CrossRef](#)]
107. Kimura, T.; Nakamoto, T. Microstructures and mechanical properties of A356 (AlSi7Mg0.3) aluminum alloy fabricated by selective laser melting. *Mater. Des.* **2016**, *89*, 1294–1301. [[CrossRef](#)]
108. Gong, H.; Rafi, K.; Gu, H.; Ram, G.J.; Starr, T.; Stucker, B. Influence of defects on mechanical properties of Ti–6Al–4V components produced by selective laser melting and electron beam melting. *Mater. Design* **2015**, *86*, 545–554. [[CrossRef](#)]
109. Tan, H.; Wong, E.; Dalgarno, W. An overview of powder granulometry on feedstock and part performance in the selective laser melting process. *Addit. Manuf.* **2017**, *18*, 228–255. [[CrossRef](#)]
110. Meier, H.; Haberland, C. Experimental studies on selective laser melting of metallic parts. *Mat.-Wiss. U. Werkst.* **2008**, *39*, 665–670. [[CrossRef](#)]
111. Mercelis, P.; Kruth, J.P. Residual stresses in Selective Laser Sintering and Selective Laser Melting. *Rapid Prototyp. J.* **2005**, *12*, 109–131. [[CrossRef](#)]
112. Yadroitsev, I.; Matope, S.; Dimitrov, D.; Mugwagwa, L. Investigation of the effect of scan vector length on residual stresses in selective laser melting of maraging steel 300. *S. Afr. J. Ind. Eng.* **2019**, *30*, 60–70.
113. Zaeh, M.F.; Branner, G. Investigations on residual stresses and deformations in selective laser melting. *Prod. Eng.* **2010**, *4*, 35–45. [[CrossRef](#)]
114. Kempen, K.; Vrancken, B.; Thijs, L.; Bols, S.; Van, H.J.; Kruth, J.P. Lowering thermal gradients in selective laser melting by pre-heating the baseplate. In Proceedings of the Solid Freeform Fabrication Symposium Proceedings, Austin, TX, USA, 12–15 August 2023; pp. 12–14.
115. Mugwagwa, L.; Yadroitsev, I.; Matope, S. Effect of process parameters on residual stresses, distortions, and porosity in selective laser melting of maraging steel 300. *Metals* **2019**, *9*, 1042. [[CrossRef](#)]
116. Thomas, B.R.; Bibb, R. An investigation into the geometric constraints of selective laser melting for the development of design rules. In Proceedings of the 9th National Conference on Rapid Design, Prototyping & Manufacture, High Wycombe, UK, 13 June 2008; pp. 11–20.

117. Yadroitsev, I.; Yadroitsava, I.; Bertrand, P.; Smurov, I. Factor analysis of selective laser melting process parameters and geometrical characteristics of synthesized single tracks. *Rapid Prototyp. J.* **2012**, *12*, 201–208. [[CrossRef](#)]
118. Thijs, L.; Verhaeghe, F.; Craeghs, T.; Van, H.J.; Kruth, J.P. A study of the microstructural evolution during selective laser melting of Ti-6Al-4V. *Acta Mater.* **2010**, *58*, 3303–3312. [[CrossRef](#)]
119. Gu, H.; Gong, H.; Pal, D.; Rafi, K.; Starr, T.; Stucker, B. Influences of energy density on porosity and microstructure of selective laser melted 17-4PH stainless steel. In *Proceedings of the Annual International Solid Freeform Fabrication Symposium*; University of Texas at Austin: Austin, TX, USA, 2013.
120. Delgado, J.; Ciurana, J.; Rodríguez, C.A. Influence of process parameters on part quality and mechanical properties for DMLS and SLM with iron-based materials. *Int. J. Adv. Manuf. Technol.* **2012**, *60*, 601–610. [[CrossRef](#)]
121. Pazon, C.; Mishurova, T.; Evsevlev, S.; Dubiez-Le Goff, S.; Murugesan, S.; Bruno, G.; Hryha, E. Residual stresses and porosity in Ti-6Al-4V produced by laser powder bed fusion as a function of process atmosphere and component design. *Addit. Manuf.* **2021**, *47*, 102340. [[CrossRef](#)]
122. Kruth, J.P.; Deckers, J.; Yasa, E.; Wauthlé, R. Assessing and comparing influencing factors of residual stresses in selective laser melting using a novel analysis method. *Proceedings of the institution of mechanical engineers. Part B J. Eng. Manuf.* **2012**, *226*, 980–991. [[CrossRef](#)]
123. Casavola, C.; Campanelli, S.L.; Pappalettere, C. Preliminary investigation on distribution of residual stress generated by the selective laser melting process. *J. Strain Anal. Eng. Des.* **2009**, *44*, 93–104. [[CrossRef](#)]
124. Weller, C.; Kleer, R.; Piller, F.T. Economic Implications of 3D Printing. *Int. J. Prod. Econ.* **2015**, *3*, 303–312.
125. Franchitti, S.; Borrelli, R.; Pirozzi, C.; Carrino, L.; Polini, W.; Sorrentino, L.; Gazzero, A. Investigation on Electron Beam Melting: Dimensional accuracy and process repeatability. *Vacuum* **2018**, *157*, 340–348. [[CrossRef](#)]
126. Abedi, R.; Hanzaki, Z.; Azami, M.; Kahnooji, M.; Rahmatabadi, D. The high temperature flow behavior of additively manufactured Inconel 625 superalloy. *Mater. Res. Express* **2019**, *6*, 116514. [[CrossRef](#)]

**Disclaimer/Publisher's Note:** The statements, opinions and data contained in all publications are solely those of the individual author(s) and contributor(s) and not of MDPI and/or the editor(s). MDPI and/or the editor(s) disclaim responsibility for any injury to people or property resulting from any ideas, methods, instructions or products referred to in the content.